Lung Imaging in the Mouse with SWIFT

C. A. Corum[1,2], D. Idiyatullin[1], S. Moeller[1], R. Chamberlain[1], D. Sachdev[2,3], and M. Garwood[1,2]

[1]Center for Magnetic Resonance Research, Dept. of Radiology, Medical School, University of Minnesota, Minneapolis, MN, United States, [2]Masonic Cancer Center, Medical School, University of Minnesota, Minneapolis, MN, United States, [3]Department of Medicine, Medical School, University of Minnesota, Minneapolis, MN, United States

Introduction: Lung and especially lung parenchyma are difficult to image with MRI[1]. T_2^* times are in the sub-millisecond range and may require specialized hardware and methods for optimum visualization or quantitative information[1,6-8]. Many lung pathologies such as inflamation (asthma), primary and metastatic neoplasms (cancer) would benefit from robust and high SNR methodologies. For example Kuethe et al.[2] have shown excellent results in rat lung with an optimized radial FID based sequence. We demonstrate here, for the first time, free breathing prospectively gated ^{1}H SWIFT images of the mouse lung. Lung parenchyma has significant signal and information content while bronchi appear dark.

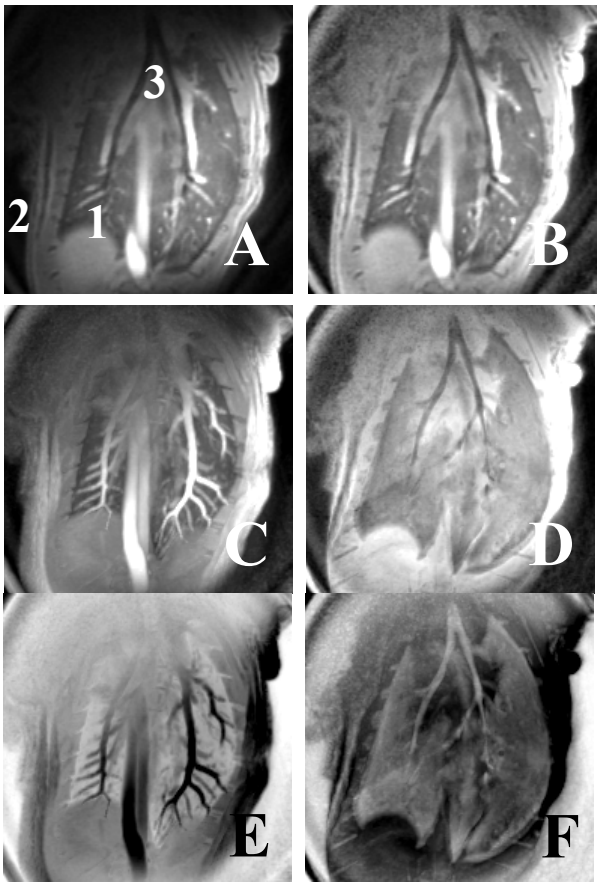

Methods: SWIFT is a novel 3D radial imaging sequence utilizing gapped frequency-swept pulse excitation and nearly simultaneous signal acquisition in the time between the gaps[3,4]. SWIFT utilizes the correlation method[5] which removes phase differences due to the time of excitation and produces FID data (k-space spokes) as if the spokes were simultaneously excited by a short duration pulse. SWIFT has an intrinsically short dead-time, at present hardware-limited to ~2-4 μs. This provides sensitivity to very fast relaxing spins (short T_2 or T_2^*) similar to BLAST/RUFIS or UTE (Ultra-short TE) sequences [2,6-8].

We placed nude mice (~25g), anesthetized with 1.5% Isoflurane, Oxygen, Nitrous Oxide mixture, with respiratory pressure sensor pad under abdomen and rectal thermocouple (SAII), prone in our 9.4 T 31 cm bore animal magnet (Varian Inova/Magnex). We used a custom built water heated holder and quadrature surface coil with two ~2 cm loops (approximate sizes 3 cm x, 1cm y, 2 cm z) just back of the shoulder over the dorsal surface of the spine. Prospective gating was accomplished by attaching the SAII 1025 gating module to the console. The gating window and delay was adjusted for acquisition efficiency once animal respiration stabilized, although was not adaptively updated.

In all image datasets the bandwidth (for excitation of RF base-band and data acquisition) was 125 kHz. Each 3d radial ^{1}H SWIFT dataset consists of 128,000 unique FID views (spokes). The transmit duty cycle of the excitation Hyperbolic Secant pulse[4] was 25%. TR was 2.9 ms with 2.048 ms of 50% duty cycle acquisition time included. The FOV was ellipsoidal 3x3x4 cm. Nominal resolution is 0.12x0.12x0.16 mm. Total time for each image was 12 min. including steady state scans and gating. Gating was accomplished in a series of 150 views per respiration cycle and respiration was at ~40 per min. Equivalent ungated images would be 6 min. for about 50% percent efficiency. We combined data from 4 acquisitions (total time 48 min) together into one final image. Processing of the SWIFT data was accomplished by in house LabVIEW (National Instruments) software consisting of correlation with the RF shape file, automatic phasing, dc estimation, and data driven distortion correction[9-10]. The radial reconstruction was accomplished by in house gridding utilizing multi-threaded "ifort" (Intel) code with 3x over-sampled width=4 Kaiser-Bessel kernel and grid once density weighting[11].

Results and Discussion: Here we present a series of images summarizing the results. So far 3 animals have successfully been imaged with the method. Figure A shows a slice along the main bronchial branch from a combined dataset. In all images the slice is in the same position. SNR (4x4x1 signal ROI parenchyma at Position 1 over 4x4x1 noise ROI at left Position 2) is 50-75 and signal level of the parenchyma is 2/3 of the nearby diaphragm. Figure B is the same image but with intensity flattening to partially remove the surface coil induced intensity differences (the image was divided by a 20 pixel radius Gaussian blurred image, with constant added). Inflow contrast is seen in the large vessels, the large bronchi are black, and significant signal is obtained from the lung parenchyma. Figure C shows a 16 slice MIP which brings out the vessels. In Figure D, we show a 16 slice minimum intensity projection from slightly dorsal compared to figure A-C which shows bronchial branching. Figure E, inverts the intensity scale of figure C. Note that there is some cardiac related motion smearing in all images at Position 3, as these datasets were not cardiac gated. Figure F is an inverted intensity scale version of figure D, which highlights that lung parenchyma signal, while lower than other surrounding tissues, is significant and contains much information such as contrast from small vessels and small bronchi.

SWIFT has some unique properties compared to pure FID based sequences. SWIFT does not lose the dc k-space information inside the pulse[12] or require ramp sampling[13]. In addition SWIFT has much lower peak power requirements than BLAST/RUFIS which allows SWIFT to be used for human imaging[4]. For these reasons we feel SWIFT has great potential for human and animal lung imaging, including inflammation and cancer.

Acknowledgments: We gratefully acknowledge NIH BTRR - P41 RR008079, Masonic Cancer Center startup funds (to DS) and The Keck Foundation. We also acknowledge Gregor Adriany for the 9.4 T coil and J. Kulesa, R. Zhou, H. Zhang, and J. Zhong for help and experience with the SAII system.

1 Beckmann, N.; Tigani, B.; Mazzoni, L. & Fozard, J. R. MRI of lung parenchyma in rats and mice using a gradient-echo sequence. *NMR Biomed,* **2001**, *14*, 297-306
2 Kuethe, D. O.; Adolphi, N. L. & Fukushima, E. Short data-acquisition times improve projection images of lung tissue. *Magn Reson Med,* **2007**, *57*, 1058-1064
3 Idiyatullin, D.; Corum, C.; Park, J. Y. & Garwood, M. Fast and quiet MRI using a swept radiofrequency. *J Magn Reson,* **2006**, *181*, 342-349
4 Idiyatullin, D.; Corum, C.; Moeller, S. & Garwood, M. Gapped pulses for frequency-swept MRI. *J Magn Reson,* **2008**
5 Dadok, J. & Sprecher, R. F. Correlation NNW spectroscopy *Journal of Magnetic Resonance (1969),* **1974**, *13*, 243-248
6 Bergin, C. J.; Pauly, J. M. & Macovski, A. Lung parenchyma: projection reconstruction MR imaging. *Radiology.,* **1991**, *179*, 777-781
7 Fast imaging in liquids and solids with the Back-projection Low Angle ShoT (BLAST) technique. *Magn Reson Imaging,* **1994**, *12*, 1047-1051
8 Madio, D. P. & Lowe, I. J. Ultra-fast imaging using low flip angles and FIDs. *Magn Reson Med,* **1995**, *34*, 525-529
9 Corum, C. A.; Moeller, S.; Idiyatullin, D. & Garwood, M Signal Processing and Image Reconstruction for SWIFT *Proceedings 15th Scientific Meeting, ISMRM,* **2007**, 1669
10 Moeller, S et al. Correction of RF pulse distortions, with application in radial imaging using SWIFT *Proceedings 16th Scientific Meeting, ISMRM, Toronto,* **2008**, 229
11 Jackson, J.; Meyer, C.; Nishimura, D. & Macovski, A. Selection of a convolution function for Fourier inversion using gridding *IEEE Transactions on Medical Imaging,* **1991**, *10*, 473- 478
12 Kuethe, D. O.; Caprihan, A.; Lowe, I. J.; Madio, D. P. & Gach, H. M. Transforming NMR data despite missing points. *J Magn Reson,* **1999**, *139*, 18-25
13 Robson, M. D.; Gatehouse, P. D.; Bydder, M. & Bydder, G. M. Magnetic resonance: an introduction to ultrashort TE (UTE) imaging. *J Comput Assist Tomogr,* **2003**, *27*, 825-46